THE JOURNAL OF PHYSICAL CHEMISTRY C

Article

Cite This: J. Phys. Chem. C 2019, 123, 12276−12285

pubs.acs.org/JPCC

Adsorption of Gadolinium (Gd^{3+}) Ions on the Dibenzo Crown Ether (DBCE) and Dicyclo Hexano Crown Ether (DCHCE) Grafted on the Polystyrene Surface: Insights from All Atom Molecular Dynamics Simulations and Experiments

Praveenkumar Sappidi,[†] Anil Boda,[‡] Sk. Musharaf Ali,[‡] and Jayant K. Singh*[,†]

[†]Computational Nano Science Laboratory, Department of Chemical Engineering, Indian Institute of Technology (IIT) Kanpur, Kanpur 208016, India

[‡]Chemical Engineering Division, Bhabha Atomic Research Center, Mumbai, India 400085

Supporting Information

ABSTRACT: All atom molecular dynamics simulations and experiments were performed to understand the adsorption behavior of gadolinium (Gd^{3+}) ion on the crown ethers grafted polystyrene (PS) surface. Two different types of crown ethers, viz., dibenzo crown ether (DBCE) and dicyclo hexano crown ether (DCHCE), were grafted separately on the PS surface to understand the adsorption behavior. We investigate the roles of Gd^{3+} ion concentration and grafting density (ρ_s) of the crown ether on the adsorption behavior of Gd^{3+} ion on the PS surface. The adsorption of Gd^{3+}shows an increasing trend with increasing salt concentration, for all cases of crown ether grafting densities. The adsorption behavior follows the Langmuir isotherm model. The maximum amount of Gd^{3+} ion adsorption was observed to be 1.83 mg/g for DBCE and 2.02 mg/g for DCHCE at ρ_s = 2.07 mol/nm^2. The maximum amount of Gd^{3+} ion adsorption on DBCE coated PS beads, in batch experiments, was found to be 1.76 mg/g, which is in good agreement with the theoretical results. The increase in ρ_s from 0.25 to 2.07 mol/nm^2 shows an increase in the q_{max} value by ∼422% and 329% for DBCE and DCHCE, respectively. The optimum value of the crown ether grafting density is found to be 1.25 mol/nm^2, beyond which the q_{max} saturates. We further investigate the dynamics of the Gd^{3+} ion by evaluating the diffusion coefficient (D) and mean residence time (τ). It was found that D decreases with increasing salt concentration for both DBCE and DCHCE. On the contrary, as expected, the τ value of Gd^{3+} increases with an increase in salt concentration. Overall, a 3-fold increase in τ was seen with increasing salt concentration. The potential of mean force analysis using umbrella sampling reveals favorable binding energy for higher grafting density of DCHCE compared to that of DBCE.

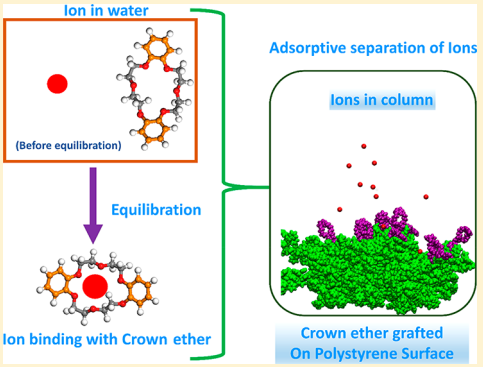

1. INTRODUCTION

Nuclear waste contains heavy metal ions such as lanthanides and actinides. Removal of gadolinium (Gd^{3+}) from the wastewater is of immense interest due to several applications of gadolinium. Natural gadolinium forms seven stable isotopes, viz., ^{152}Gd, ^{154}Gd, ^{155}Gd, ^{156}Gd, ^{157}Gd, ^{158}Gd, and ^{160}Gd.[1] Gadolinium possesses a maximum cross section as 254 000 b (barn) for Gd-157 and 60 900 b for Gd-155. This specific property augmented that both Gd-157 and Gd-155 were efficiently being used as burnable poison in nuclear fuel. Hence, separation of Gd isotopes has a very important role in the nuclear reactor operation.[2] For example, Gd-152 is used for bone density measurement in the osteoporosis research. Gd is also the most commonly used metal for magnetic resonance imaging (MRI) contrasting agents.[3] Due to extensive usage of Gd as a contrasting agent in the diagnostics and as a nuclear fuel, the removal of Gd from the spent nuclear fuel and biomedical waste is warranted due to environmental concerns.[3]

Generally, heavy metal ions are known to be toxic and separation of heavy metal ions from aqueous waste is a challenging task. Hence, Gd^{3+} ions are imperative to be removed from wastewater streams.[4] In the recent past, various methods have been proposed for the separation of Gd^{3+} such as cloud point extraction,[5] solvent exraction,[6] nanofiltrations,[7] solid−liquid extraction,[7−10] and column chromatography.[11,12] Among them, solvent extraction is a widely used method for the separation of metal ions.[13] In this method, an extractant plays a vital role to extract a metal ion from an aqueous phase to an organic phase. The macrocyclic polyethers (crown ethers) described by Pedersen[14] are of particular interest because of their remarkable complexing properties as an extractant. These compounds form a variety of complexes with many cations, both in solution and in the crystalline states. In the complex of a typical polyether, such as 18-crown-6, the cation is located in the center of the hydrophilic cavity which is surrounded by the electronegative oxygen atoms and the

Received: February 22, 2019
Revised: April 20, 2019
Published: April 23, 2019

DOI: 10.1021/acs.jpcc.9b01722
J. Phys. Chem. C 2019, 123, 12276−12285

cation is held by ion-dipole forces.[15,16] Due to the special type of complexation of metal ions, the crown ethers have gained significant interest in the field of separation science and technology. Earlier studies indicate that the crown ethers such as dibenzo crown ether (DBCE) and dicyclo hexano crown ether (DCHCE) are good candidates for the favorable binding of Gd^{3+} ions.[11,12] Previous experiments and theoretical studies[11] have reported that both the DBCE and DCHCE form a complexation with a Gd^{3+} ion in the gas phase and solvent phase. However, crown ether compounds have some drawbacks as these are difficult to recover, toxic in nature, and solubility loss in various solvents. Hence, the resulting reaction mixture can cause an environmental issue. This drawback can be reduced by grafting crown ethers on soft (polymer) or hard material (carbon based materials).[17] Solid substrate based extraction methods are attractive lately as they are economical and environmentally less harmful. For example, the adsorption based process produces less secondary pollutant and also utilizes less solvent compared to other traditional extraction methods. Thus, it has been widely utilized in separation and preconcentration of elements from environmental samples. There is increased attention in recent days on the use of immobilized crown ethers on the separation of heavy metal ions. The use of immobilized crown ethers such as grafting the crown ethers on the surface of polymeric material would be effective in the removal of metal ions and further regeneration of crown ether.[18] These types of materials would effectively reduce the environmental concerns, as these materials provide ease of handling and recoverability. Furthermore, crown ethers grafted with polymer show an enhanced separation capability of heavy metal ions as seen by previous experiments.[18,19]

The UV/vis study by Gao et al.[20] on the immobilized DBCE on the surface of polyvinyl alcohol (PVA) has shown higher adsorption capabilities for the metals in the order of Zn^{2+} > Co^{2+} > Cd^{2+} > Cu^{2+} > Ni^{2+} > Pb^{2+}. The spectroscopic and theoretical studies[21,22] have shown that the grafting of crown ether on the poly(methyl methacrylate) enhances binding of the various lanthanide ions such as terbium Tb^{3+}, cerium Ce^{3+} and no binding for the Gd^{3+} on the crown ether. The column chromatography study by Boda et al.[11] on DBCE grafted on the polystyrene surface has shown enhanced adsorption behavior of Gd^{3+} ions. The complexation behavior of Gd^{3+} with crown ethers has been studied theoretically in the literature.[23−26] A recent molecular simulation study from our group[27,28] has shown that an increase in the polystyrene chain length on the DBCE and DCHCE increases the binding affinity of Gd^{3+}.

Despite the above studies, there are few unanswered questions. For example, the effect of chemically different crown ethers (DBCE and DCHCE), grafted on the surface of polystyrene, on the adsorption behavior of Gd^{3+} is not studied. What would be the role of grafting density, ρ_s, of the crown ether on the adsorption of Gd^{3+} ions? Is there an optimum value of grafting density which yields a maximum amount of adsorption of Gd^{3+} ions? This article aims to address the above questions.

In particular, we present an atomistic molecular dynamics simulations study to understand the Gd^{3+} adsorption behavior on the polystyrene surface grafted with DBCE and DCHCE. The column chromatography experiments are performed to validate the observed theoretical observations. The rest of the article is organized as follows: Section 2 describes the molecular models, simulation, and experimental procedures adopted in this study. Section 3 presents the results and discussion, followed by conclusions in section 4.

2. METHODS

2.1. Modeling and Simulation Details. The crown ethers DBCE, DCHCE and an *atactic* polystyrene (PS) chain of 20 repeat unit are generated using Material Studio.[29] Density Functional Theory calculations are performed on both DBCE and DCHCE to optimize the molecular geometry using B3LYP/6-31G(d,p) as implemented in the Gaussian 09.[30] The optimized molecules of DBCE and DCHCE are grafted randomly on the surface of the polymer. The OPLS force field is used for all the molecules such as DBCE, DCHCE, PS, HNO_3, Gd^{3+}, and NO_3 for the all atom molecular dynamics simulations.[31] The details of all the bonded and nonbonded interactions are presented in the previous work.[27,28] We have used the TIP3P water model,[32] and the acidic medium (1 M) is maintained by considering H_3O^+ and NO_3^- ions in an aqueous solution. The particle mesh Ewald (PME)[33] is used for calculating the electrostatic interactions with a 1 nm cutoff radius with a grid spacing of 0.1 nm and an interpolation order of 4. The Lennard-Jones 6-12 potential is used for calculating the van der Waals interactions with a 1.4 nm cutoff radius. All the bond lengths are constrained using the LINCS method.[34] A Nose−Hoover thermostat and Parrinello−Rahman barostat are used, respectively, for maintaining the temperature at 300 K, with a coupling constant τ_t = 0.5 ps, and the pressure at 1 atm, with a coupling constant τ_p = 0.5 ps. The compressibility of water of about 4.5 × 10^{-10} kPa^{-1} is considered. The equation of motion is solved using the leapfrog algorithm with a 2 fs time step. The steepest-decent method is used for all potential energy minimization. All simulations are performed using the Gromacs 4.5.5.[35]

In the first step, we created an amorphous polymer surface equivalent to the experimental density.[36] To that end, we performed a simulation of 20 repeat units of a single PS chain in water in an 8 nm cubic box, 100 ps NVT and 100 ps NPT simulations, followed by 20 ns NPT-MD simulations using the periodic boundary conditions in the *x*, *y*, and *z* directions. The equilibrated chain is used for the generation of multiple polymer chains, by placing the chains, 50 in number, randomly in the box of 12 × 12 × 9 nm in size. Subsequently, we have performed NPT-MD simulation for 50 ns at a temperature of 600 K using periodic boundary conditions in all the directions. Figure S1 in the Supporting Information (SI) presents the snapshots of PS aggregation. During the equilibration process, the polystyrene chains are found to aggregate and form an amorphous polymer melt after equilibration. The box dimension for this amorphous polymer sample is enlarged for 20 nm in the *z* direction to provide a vacuum slab on top of the aggregated polymeric surface. The NVT-MD simulations are performed for this enlarged system for another 20 ns in order to generate the smooth polymer surface as shown in Figure 1. We observed that 20 ns runs are sufficient for the density of 0.911 g/cm^3, similar to the experimental density of 0.914 g/cm^3.[36] This procedure is identical to the method adopted in the literature.[37] After the equilibration, the temperature of the simulated system is cooled to a temperature of 300 K at the rate of 0.01 K/ps. The final amorphous surface has a thickness of ∼4 nm, the final box dimensions of the surface as 7.06 × 7.06 × 3.7 nm.

The optimized DBCE molecules are grafted on the equilibrated polystyrene surface. This is achieved by randomly

DOI: 10.1021/acs.jpcc.9b01722
J. Phys. Chem. C 2019, 123, 12276−12285

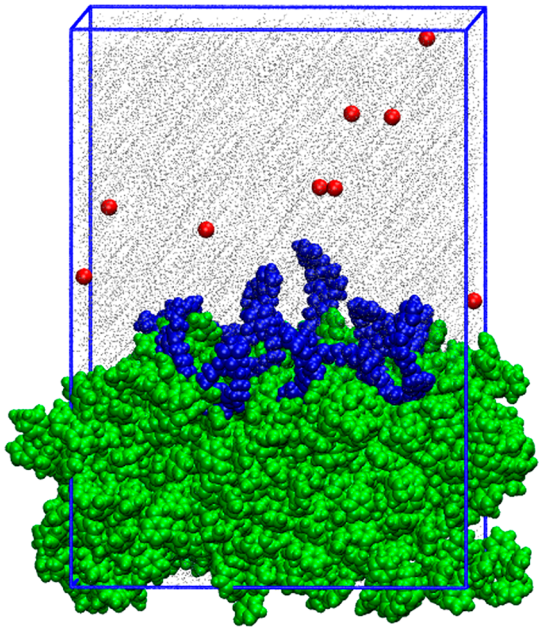

Figure 1. Initial simulation setup at grafting density 1.0 mol/nm^2 on the surface of the polystyrene. Color codes: Green, polystyrene; blue, crown ether (DBCE); red, gadolinium (Gd^{3+}) ions; and gray, water molecules.

replacing the para hydrogens of the polystyrene ring by using the methylated bond to make sure that DBCE molecules are exposed to the z direction. We created seven grafted surfaces by grafting 3, 6, 9, 12, 15, 20, and 25 DBCE molecules randomly. These grafted surfaces correspond to the grafting density: 0.24, 0.49, 0.74, 1.00, 1.25, 1.66, and 2.07 mol/nm^2, respectively, for 3, 6, 9, 12, 15, 20, and 25 DBCE molecules. Figure 1 presents a snapshot of the crown ether grafted system. A similar procedure is used for generating the grafting DCHCE on the substrate.

The generated DBCE and DCHCE grafted substrates are used as starting structures for investigating the adsorption behavior of the Gd^{3+} in water. The box dimension in the z direction is extended by ~2.7 times to fill with the bulk water. The water molecules and salt ions are added above the polymer surface. The $Gd(NO_3)_3$ concentration is varied in the range, 0.05−0.5 M. Figure 2 presents the initial density distribution of all the molecules present in the simulation system for two cases, viz., with and without grafted crown ethers. The vacuum slab of 20 nm is added on the above prepared system to avoid the effect of the periodic image. We performed NVT-MD simulation of run length 40 ns on the above systems to observe the adsorption behavior. The last 10 ns run is used to analyze the structural and thermodynamical properties.

Umbrella Sampling (US) is performed using a harmonic biased potential, as shown in eq 1, to understand the free-energy barriers associated with the ion binding structure in the gas phase and in water.

$$w_i(\xi) = \frac{1}{2}k(\xi - \xi_i)^2 \tag{1}$$

Here, ξ is the distance between the center of mass of the crown ether and Gd^{3+} ion (only one ion). ξ is the only collective variable (CV) we have considered in this work. ξ_i is the variation in the reaction coordinate from the DBCE or DCHCE grafted on the PS, and k is biasing force constant, which provides a good overlap in between neighboring sampling windows. There are no additional ions present in the simulation system, except the counterions (NO_3^-) and other solvent molecules, which are placed randomly in the simulation box. The Gd^{3+} is restrained using a harmonic potential with a force constant of 1000 (kJ/mol nm^2) along the normal to the center of mass of DBCE and DCHCE. The potential of mean force (PMF) is calculated using the Weighted Histogram Analysis Method (WHAM)[38,39] as implemented in Gromacs.[40] The detailed information on the WHAM method is provided in the SI. A 0.1 nm window spacing is used for the sampling of the windows along with the reaction coordinate with a 10 ns simulation time for each window. We have performed simuations with 23 widows for each case, viz., DBCE-Gd^{3+} in (1) water, (2) vacuum, and DCHCE-Gd^{3+} in (3) water, and (4) vacuum. Thus, a total of 92 (4 × 23) simulations are performed.

Adsorption analysis of Gd^{3+} ions on the surface of the polystyrene surface is calculated using the Langmuir isotherm model given by

$$q_e = \frac{q_{max}KC}{1 + KC} \tag{2}$$

where q_e is defined as the amount of Gd^{3+} adsorbed per unit mass of crown ether (mg/g). The q_{max} (mg/g) is defined as the maximum possible amount of Gd^{3+} ions adsorbed, K is the Langmuir model constant, and C (mol/L) is the equilibrium metal ion concentration. The essential feature of the Langmuir model is described using the Langmuir equilibrium parameter R_L, which can be calculated using the relation:

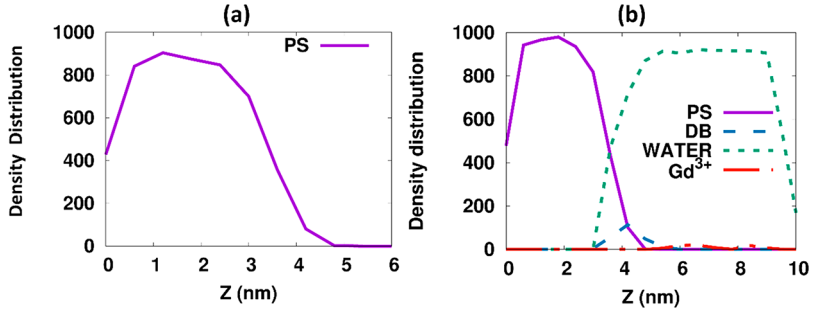

Figure 2. Density distribution along the Z direction of initial simulation setup for 0.05 M $Gd(NO_3)_3$ at ρ_s = 0.25 mol/nm^2 (a) without crown ether grafting and (b) with crown ether grafting.

DOI: 10.1021/acs.jpcc.9b01722
J. Phys. Chem. C 2019, 123, 12276−12285

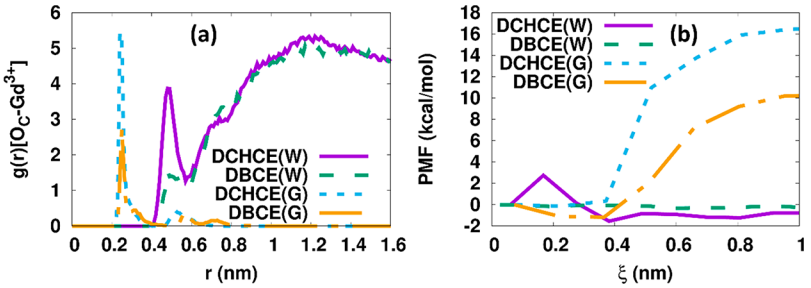

Figure 3. (a) Radial distribution function of O_C and Gd^{3+} in water and in vacuum for DBCE and DCHCE, and (b) PMF curves for the ion binding energy along the z direction. Here, symbols W and G represent water and vacuum, respectively. Overall free-energy values in each case show a standard error of approximately 1%.

$$R_L = \frac{1}{1 + KC} \tag{3}$$

The self-diffusion coefficient (D) of the Gd^{3+} ions is calculated using the relation[28]

$$D = \frac{1}{6t}\lim_{t\to\infty}\langle ||r_i(t) - r_i(0)||^2\rangle_{i\in A} \tag{4}$$

where $r_i(t)$ is the center-of-mass position vector of the Gd^{3+} ion at a time "t".

2.2. Batch Adsorption Experiments. The detailed synthesis and characterization procedures of CMPS-DB18C6 resin is given elsewhere.[11] The batch experiments are conducted with the synthesized CMPS-DB18C6 resin for Gd^{3+} ions by varying the concentration of metal ions at pH 5.0. The 1.0 g of each CMPS-DB18C6 is weighed and poured into a glass bottle of 20 mL volume. The $Gd(NO_3)_3$ solution of (10 mL) is added slowly to represent the concentrations varying from 10 to 500 ppm. This entire mixture is subjected to shaking at the rate of 300 rpm for 4 h at the room temperature in an incubator orbital shaker (IKA KS 4000). The inductively coupled plasma optical emission spectroscopy (ICP-OES) by Horiba Scientific (Jobin Yvon Ultima 2) is used to determine the liquid phase concentration of Gd^{3+} ions after the mixture attained an equilibrium. These experiments are repeated two times, and the average properties of two tests are considered. The amount of adsorption capacity at equilibrium, q_e (mg/g), is calculated using the following equation[11]

$$q_e = (C_0 - C_e) \times \frac{V}{m} \tag{5}$$

where C_o is the initial concentration and C_e is the equilibrium ion concentrations of Gd^{3+} in (mg/L), V is the initial solution volume in (liters), and m (g) is the mass of the adsorbent added to the solution.

3. RESULTS AND DISCUSSION

3.1. Gd^{3+} Binding Structure. Gd^{3+} ion binding structure is calculated by evaluating the radial distribution function (RDF) between Gd^{3+} ions and oxygens of the crown ether (O_C) for both DBCE and DCHCE. Figure 3a,b presents the RDF plot of O_C and Gd^{3+}, and PMF of O_C and Gd^{3+}, respectively. The O_C-Gd^{3+} first peak is located at 0.24 nm in the gas phase and 0.48 nm in water for both DBCE and DCHCE. The peak intensity is higher for Gd^{3+}-O_C of DCHCE compared to DBCE, both in the gas phase and in water. This particular behavior is in good agreement with the previous gas phase theoretical results reported by Boda et al.,[11] where the binding distance of 0.24 nm between Gd^{3+} and O_C of DBCE is reported. The previous simulation studies[27,28] have shown the Gd^{3+} binding distance as ∼0.24 nm for both DBCE and DCHCE, where it is considered as a precomplexed structure as Gd^{3+}-DBCE and Gd^{3+}-DCHCE. However, in the present work, the binding distance between O_C-Gd^{3+} in water is ∼0.48 nm, which is 2 times higher than that in the gas phase. In this work, we have considered an explicit description of all the ions and solvent molecules, which exhibits a significant intermolecular interaction between the Gd^{3+} ion, solvent molecules, and other counterions present in the simulation system. The gas phase simulation study[7] reported that the Gd^{3+} ion-DCHE binding energy is approximately 2 times higher than the Gd^{3+} ion-DCHE binding energy. The more prominent peak in the RDF of the pair Gd^{3+}-O_C of DCHCE indicates that a difference in the structure of crown ether when compared to the DBCE change in the crown ether can show a moderate difference on the binding behavior of Gd^{3+} with the crown ether. The presence of double bonds on the benzene ring makes the structure of DBCE more stable than that of the cyclohexane ring on DCHCE, which enhances the binding ability of Gd^{3+} with DCHCE.

To understand the differences between the binding structural properties in the gas and solvent phases, we have calculated the potential of mean force (PMF) using the umbrella sampling. Figure 3b presents the PMF curves for the Gd^{3+} ions for both DCHCE and DBCE in the gas and solvent phases. In the case of Gd^{3+}-DBCE, the free-energy minimum is found to be −1.02 kcal/mol at ξ = 0.22 nm in the gas phase and −0.42 kcal/mol at ξ = 0.48 nm in the solvent phase. Similarly, for Gd^{3+}-DCHCE, the free-energy minimum is −0.18 kcal/mol in the gas phase at ξ = 0.22 nm, and −2.02 kcal/mol at ξ = 0.48 nm in the solvent phase. This indicates that the binding of Gd^{3+} on DCHCE is more favorable in the solvent phase compared to that in the gas phase. The 2-fold higher free-energy barrier in the water compared to the gas phase is indicative of stronger binding of Gd^{3+} and oxygens of DCHCE and DBCE. On the basis of the values of PMFs, binding of Gd^{3+} follows the order: DCHCE(w) > DBCE(g) > DBCE(w) > DCHCE (g). This behavior is similar to the gas phase study[11] where the binding energy of Gd^{3+}-DCHCE is 2-fold higher than the binding energy of Gd^{3+}-DBCE. Next, we study the adsorption behavior of the ions on the crown ether grafted polystyrene surface.

3.2. Adsorption Behavior. Figure 4 presents the density profiles of Gd^{3+} ions on the grafted polymer for both DBCE and DCHCE at a grafting density, ρ_s, of 1.25 mol/nm^2. The density profiles of Gd^{3+} ions for other ρ_s values for both DBCE and DCHCE are given in Figures S2 and S3 in the SI. The profiles display a peak at ∼6 nm, which does not change with

DOI: 10.1021/acs.jpcc.9b01722
J. Phys. Chem. C 2019, 123, 12276−12285

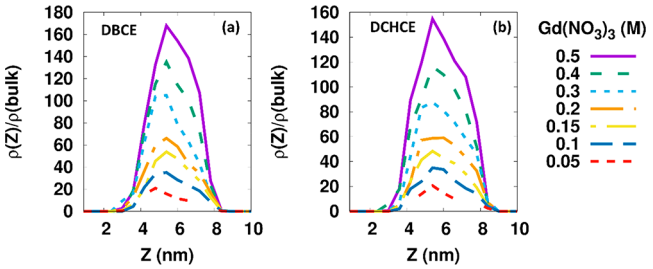

Figure 4. Density distribution of Gd^{3+} at ρ_s (1.25 mol/nm^2) for (a) DBCE and (b) DCHCE.

an increase in grafting density and salt concentration. The increase in the Gd^{3+} ion concentration enhances the peak intensity as seen for all the ρ_s, studied here. The density distribution peak spans from ∼2 nm until 6 nm, due to the thicknesses of the amorphous polymer surface (∼4 nm) and the grafted crown ethers above the polystyrene surface (∼2 nm), as it can be seen from Figure 2. The presence of the broad peak indicates that the Gd^{3+} ions show a significant binding onto the grafted crown ethers, which is found to be similar for both the DBCE and DCHCE. Figure 5 presents representative snapshots for the case of 0.5 M $Gd(NO_3)_3$ concentration at a ρ_s = 1.25 mol/nm^2 for both DBCE and DCHCE. The ions which directly bind on the crown ether first fill up the void spaces present above the PS surface; then the remaining Gd^{3+} ions start to agglomerate near the crown ethers.

To understand the adsorption behavior of the ions, we have considered a thickness of 1 nm (of Gd^{3+} ions) above the polystyrene surface. The number of metal ions adsorbed per gram of adsorbent q_e (mg/g) is calculated by first counting the number of ions adsorbed within this monolayer and then finally converting them into milligrams. Figure 6 presents the adsorption isotherm curves of Gd^{3+} ions, following the Langmuir adsorption isotherm model (eq 2). The q_e increases with an increase in grafting density for both DBCE and DCHCE. The q_e value shows an increase until ρ_s = 1.65 mol/nm^2; beyond this amount, q_e does not change significantly. However, in the case of DCHCE, we observe a slight increase in q_e at a higher grafting density of 2.07 mol/nm^2. The maximum adsorption capacity q_{max} (mg/g) and Langmuir constant K are obtained by fitting the linearized form of the Langmuir isotherm equation.

Figure 7 presents the fitted q_{max} values for different grafting density values. The q_{max} values are found to increase with an increase in the grafting density. It is also observed from the figure that increasing ρ_s beyond 1.25 mol/nm^2 does not show a significant difference. However, a further increase in the grafting density would diminish the void spaces within the grafted surface which would lower the adsorption capacity. The q_{max} values show an increase of ∼422% for DBCE and ∼329% for DCHCE with an increase in ρ_s from 0.25 to 2.07 mol/nm^2. However, in the intermediate range, 1.25 mol/nm^2 < ρ_s < 2.07 mol/nm^2, the q_{max} increases by ∼15% for DBCE and ∼16% for DCHCE. In contrast to that, in the lower grafting density range, 0.25 mol/nm^2 < ρ_s < 1.25 mol/nm^2, the q_{max} increases by ∼354% for DBCE and ∼270% for DCHCE. These observations indicate that the q_{max} show an ∼20-fold higher increase for the lower range of grafting density compared to the intermediate range of grafting density. On the basis of the aforementioned behavior of q_{max} value, we can consider ρ_s = 1.25 mol/nm^2 as the optimum value for both DBCE and DCHCE. The maximum Gd^{3+} adsorption capacity of ∼1.83 and ∼2.02 mg/g for DCHCE and for DBCE, respectively, is observed at ρ_s = 2.07 mol/nm^2 on the PS surface. Thus, the ρ_s = 1.25 mol/nm^2 value can be taken as an optimum value for maximizing the adsorption of Gd^{3+} on the

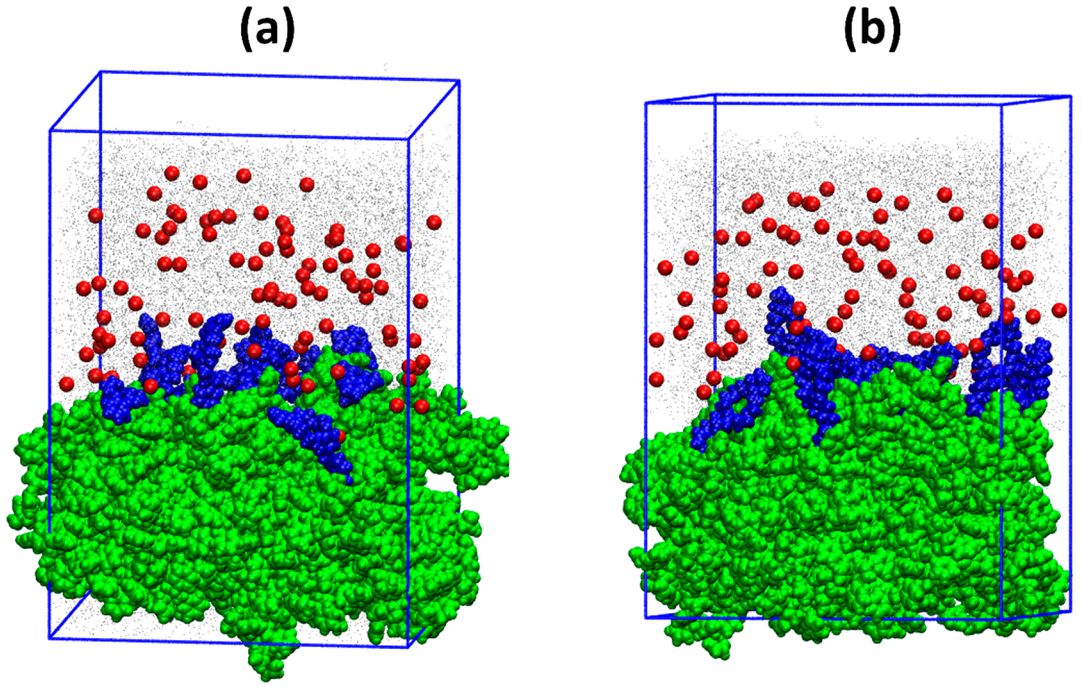

Figure 5. Simulation snapshots of amount of adsorbed Gd^{3+} ions on the surface of grafted crown ether molecules at 0.5 M $Gd(NO_3)_3$ at ρ_s = 1.25 mol/nm^2 surface for (a) DBCE and (b) DCHCE. Simulation box contains 20 nm vacuum slab above the water-filled substrate, which is not shown here for clarity.

DOI: 10.1021/acs.jpcc.9b01722
J. Phys. Chem. C 2019, 123, 12276−12285

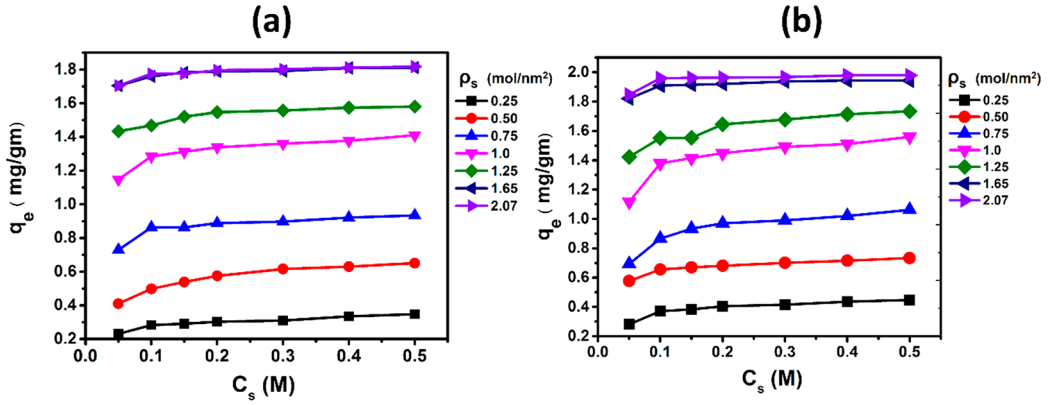

Figure 6. Amount of adsorption q_e (mg/g) for (a) DBCE and (b) DCHCE. The standard error values are within ∼4−7%.

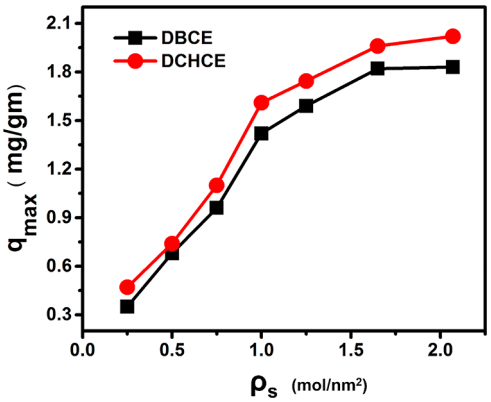

Figure 7. Maximum amount q_{max} (mg/g) of adsorption with an increase in grafting density for both DBCE and DCHCE. The standard error values vary from ∼0.3% to ∼4.4% at different ρ_s values.

DBCE and DCHCE. The q_{max} value for DCHCE is higher than that of DBCE for the entire range of ρ_s studied in this work.

Figure 8 presents the effect of grafted molecules and metal ion concentration on the Langmuir equilibrium parameter (R_L), calculated using eq 3. With an increase in the salt concentration, R_L decreases spanning in the range of 0.4−0.05, which indicates the Gd^{3+} ion adsorption becomes favorable at a higher salt concentration. The effect of grafting molecules does not show a significant influence on the R_L values for both DBCE and DCHCE ligands.

3.3. Experimental Isotherm. In order to quantitatively compare the theoretical observations, we have performed the batch adsorption experiments for a case of DBCE grafted on the polystyrene resin. The experimental adsorption capacity q_e (mg/g) of Gd^{3+} ions is calculated using eq 5. We have performed two independent batch experiments, and data for these two experiments to see the adsorption behavior; the individual run data are given as Table S1 in the SI. The average values of the two experiments are reported here; we have seen an insignificant difference in the two individual sets. Figure S4 (SI) presents the experimental isotherms fitted with the Langmuir model to obtain q_{max}. The maximum adsorption capacity q_{max} and Langmuir constant K are found to be 1.76 mg/g and 0.087, respectively. Figure 9a,b presents a comparison of experiments and simulation data of q_e (mg/g) at ρ_s = 1.25 mol/nm^2 for DBCE for simulations and DBCE coating density on PS beads as 1.18 g/cm^3. It is observed that both experiments and simulation results of q_e and R_L are qualitatively in good agreement with each other for the case of DBCE grafted on PS.

Figure 9c,d presents the equilibrium parameter R_L, using eq 3, evaluated from the experimental with increasing Gd^{3+} ion concentration, respectively. The R_L values decrease with an increase in the salt concentration, indicative of favorable adsorption of Gd^{3+} ions at a higher salt concentration. These values are in reasonable agreement with the theoretically predicted R_L values, which indicates favorable adsorption of Gd^{3+} ions with the resin.[41] Thus, our theoretical model system

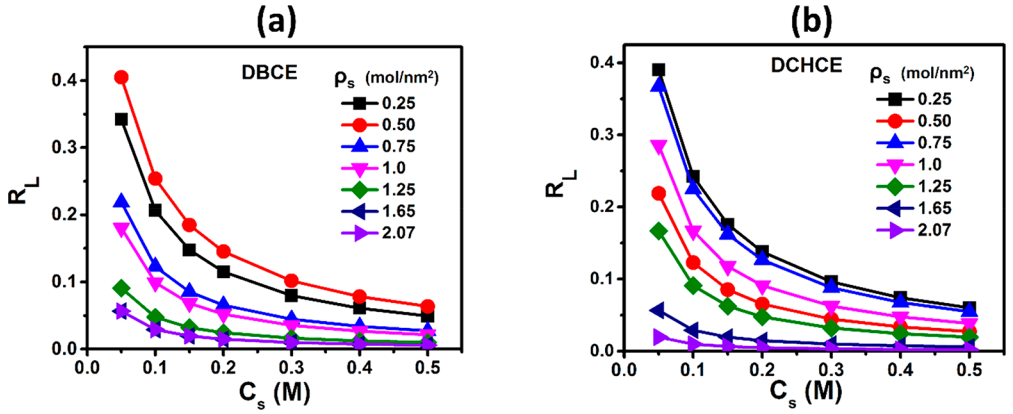

Figure 8. Equilibrium parameter (R_L), with an increase in metal ion concentration of (a) DBCE and (b) DCHCE. Here, the standard error values are within ∼4−7% .

DOI: 10.1021/acs.jpcc.9b01722
J. Phys. Chem. C 2019, 123, 12276−12285

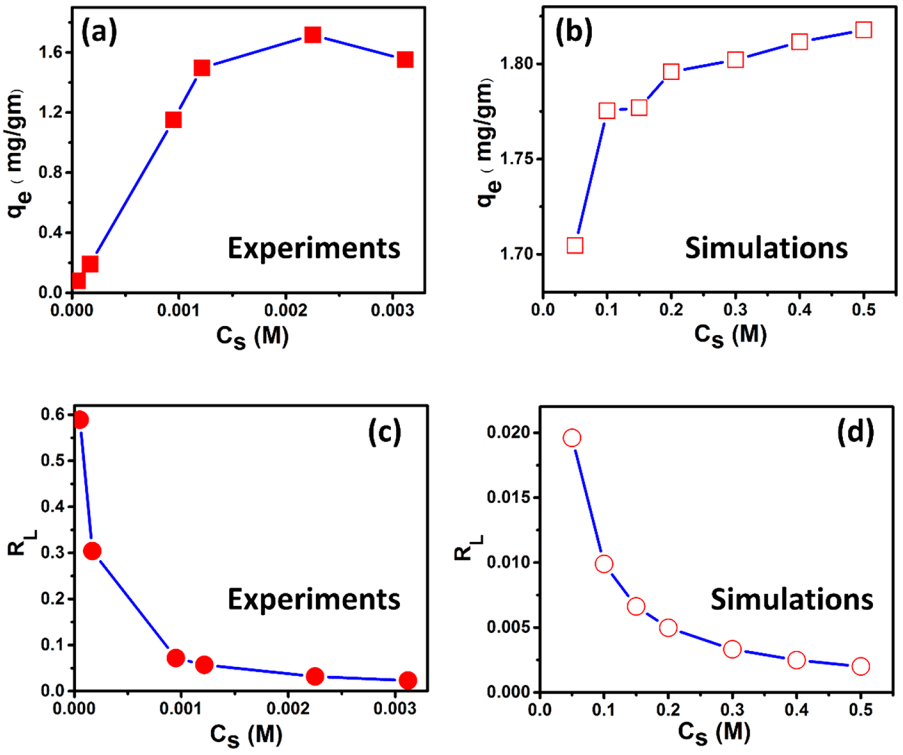

Figure 9. Amount of adsorption q_e (mg/g) for DBCE: (a) experiments, (b) simulations and the equilibrium parameter (R_L), (c) experiments, (d) simulations, with an increase in the metal ion concentration. The simulation data are taken at ρ_s = 1.25 mol/nm^2. The experiments are conducted with DBCE coating density of 1.18 g/cm^3 on PS beads.

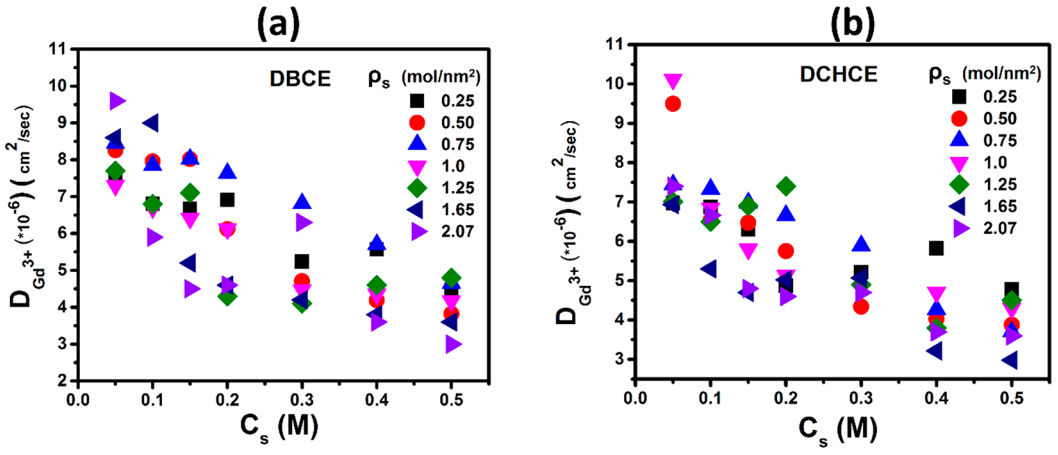

Figure 10. Self-diffusion coefficient of adsorbed Gd^{3+} ions. (a) DBCE and (b) DCHCE. The statistical errors are within ∼9% to 14%.

is able to capture the experimental adsorption behavior. The next section describes the adsorbed ion dynamics and occupational time.

3.4. Gd^{3+} Solvation and Diffusion. The Gd^{3+} ion solvation structure is calculated using the radial distribution function between water oxygen (O_W) and Gd^{3+} ions, which is presented in Figure S5 (SI). The first peak is located at 0.24 nm, which is in good agreement with previous scattering X-ray absorption experiments[42] and theoretical results.[43] The peak intensity shows an increase with an increase in Gd^{3+} ion concentration and grafting density. The observed Gd^{3+}-water coordination number values vary in the range of ∼7.9−8.6 for both DBCE and DCHCE, which is in good agreement with the literature.[42,43]

The dynamical properties of Gd^{3+} ions near the surface are also investigated, which is shown in Figure 10. Figure 10 presents the D values for both DBCE and DCHCE grafted surfaces. The observed D values are of the order of 10^{-6} cm^2/s. These values are similar to the experimental observations.[44] The D values show a decreasing trend with an increase in salt concentration. For DCHCE, the highest value of D is seen as ∼10×10^{-6} cm^2/s (at ρ_s = 1.25 mol/nm^2 and C_s = 0.05 M) and the lowest value of D is seen as 3×10^{-6} cm^2/s (at ρ_s = 1.65 mol/nm^2 and C_s = 0.5 M). It should be noted that the self-diffusion coefficient of Gd^{3+} ion in bulk water is 6×10^{-6} cm^2/s.[44] The D values observed in our simulation study are close to that of the bulk water at lower salt concentrations. On the other hand, D values at a higher salt concentration are lower than the D value in the bulk water. The D values for both

DOI: 10.1021/acs.jpcc.9b01722
J. Phys. Chem. C 2019, 123, 12276−12285

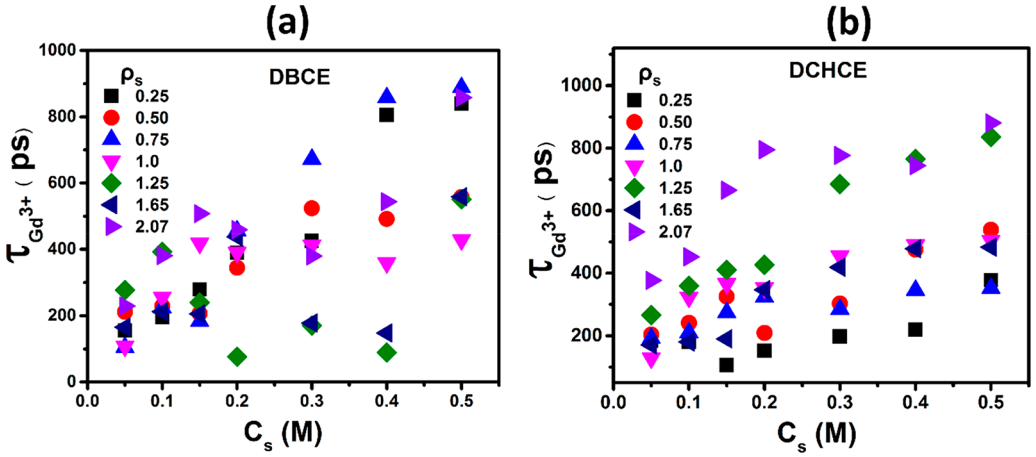

Figure 11. Residence time τ (ps) of adsorbed Gd^{3+} ions. (a) DBCE and (b) DCHCE. The standard error values vary from 5% to 7%.

DBCE and DCHCE decrease with increasing grafting density. For all the grafting densities of crown ethers (i.e., from 0.25 to 2.07 mol/nm^2), the diffusion coefficient of Gd^{3+} ions shows an ~45% decrease for DBCE and ~57% decrease for DCHCE, with an increase in salt concentration. This significant decrease in diffusion coefficient values is due to the slower mobility of the adsorbed ions on the surface of the crown ether. Furthermore, it is observed that grafting DCHCE molecules would give lower values of D for Gd^{3+} ions compared to the grafting of DBCE. Thus, it is very clear that the grafting of DCHCE significantly lowers the dynamics of adsorbed Gd^{3+} compared to the case of DBCE.

3.5. Adsorbed Gd^{3+} Ion Residence Time. Figure 11 presents the residence time τ (ps) of adsorbed Gd^{3+} ions for different ion concentrations. The τ (ps) values are calculated using an exponential fit of an occupational time correlation $C(t)$, as shown below:

$$C(t) = \frac{\langle \sum_{i=1}^{N} \varphi_i(t_0)\varphi_i(t + t_0)\rangle}{\langle \sum_{i=1}^{N} \varphi_i(t_0)\varphi_i(t_0)\rangle} \quad (6)$$

In the above equation, if the Gd^{3+} is adsorbed, then $\varphi_i(t_0)$ is taken to be 1; otherwise, it is zero. The mean residence time τ is found to increase with an increase in the ρ_s for both the grafted molecules, DBCE and DCHCE. The increase in the τ value indicates an increased affinity toward the surface of grafted molecules with increasing salt concentration. The mean residence time τ (ps) of adsorbed Gd^{3+} ions at different ρ_s (mol/nm^2) values is provided in the SI as Table S2. These values are in a similar order of magnitude of the mean residence time of lead ions (Pd^{2+}) on the polyamidoamine PAMAM dendrites grafted on the graphene.[45] Overall, more than 3 times higher values of τ is observed in going from a lower salt concentration to a higher salt concentration for both DBCE and DCHCE grafted molecules. In addition, the τ values are higher for the case of DCHCE compared to the case of DBCE, above 0.4 M, at a high grafting density of 2.07 mol/nm^2. These high τ values indicate that both DBCE and DCHCE show a maximized adsorption at higher salt concentration. The τ is higher for DCHCE when compared to DBCE beyond ρ_s = 1.25 mol/nm^2.

3.6. Potential of Mean Force. Figure 12 presents the potential mean force (PMF) with an increase in salt concentration at ρ_s = 1.25 mol/nm^2 for both DBCE and DCHCE. The PMF is calculated using PMF(z) = $-KT$ ln($\rho(z)/\rho$(bulk)). The PMF values show a decrease with an increase in the salt concentration for all the grafting densities considered in this work. The PMF curves for other ρ_s values are given in Figures S6 and S7 (SI). The most negative value of free energy (−3.23 kcal/mol) is seen at a ρ_s value of 2.07 mol/nm^2 at 0.5 M salt concentration for DCHCE. The lower values of PMF are located at a distance of 6.0 nm for both DBCE and DCHCE grafted molecules. The PMF value shows lower values for higher grafting density at a higher concentration, 0.5 M. The lower values of PMF for DCHCE compared to DBCE is indicative of the higher value of adsorption capacity. These observations are in agreement with the batch column experiments.

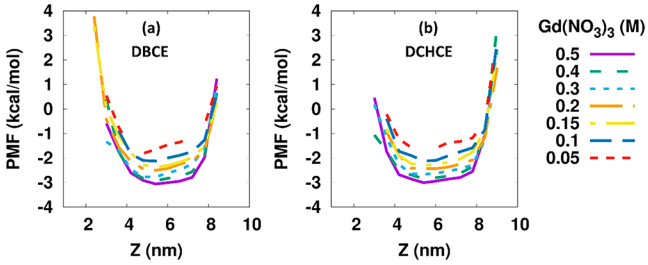

Figure 12. PMF profiles of adsorbed ions at ρ_s = 1.25 mol/nm^2. (a) DBCE and (b) DCHCE.

4. CONCLUSION

In this study, molecular dynamics simulations were performed to understand the effect of grafting density of crown ethers on the adsorption behavior of Gd^{3+} ions in the aqueous phase. The amount of adsorption shows an increase with an increase in ρ_s for both DBCE and DCHCE. The q_{max} was found to be ~1.83 mg/g for DBCE and ~2.02 mg/g for DCHCE at ρ_s = 2.07 mol/nm^2. The batch experimental study shows a q_{max} of 1.76 mg/g for DBCE, which is in good agreement with the theoretical results. Increase in grafting density increases the adsorption capacity of Gd^{3+} on the surface of the crown ether until ρ_s is 1.25 mol/nm^2, beyond which the adsorption amount saturates. In this work, ρ_s = 1.25 mol/nm^2 is found to be an optimum value of grafting density. The q_{max} value shows a rise of 422% for DBCE and 329% for DCHCE with an increase in ρ_s from 0.25 to 2.02 mol/nm^2. The D values show a 2-fold decrease with increasing ρ_s and salt concentration. The D value shows a maximum of ~45% decrease for DBCE and ~57%

DOI: 10.1021/acs.jpcc.9b01722
J. Phys. Chem. C 2019, 123, 12276−12285

decrease for DCHCE with an increase in salt concentration. The residence time of adsorbed Gd^{3+} ions shows a 3-fold increase with an increase in salt concentration. The lowest PMF values are seen for DCHCE when compared to DBCE at high grafting density. The results from this simulation study indicate that aqueous adsorption of Gd^{3+} is maximum for DCHCE when compared to the DBCE. Nevertheless, the Gd^{3+} adsorption capacity calculated by our theoretical model is able to reproduce the experimental adsorption capacity. Thus, our model is found to be suitable for estimating the adsorption capacity for similar heavy metal ions and lanthanides.

■ ASSOCIATED CONTENT

Supporting Information

The Supporting Information is available free of charge on the ACS Publications website at DOI: 10.1021/acs.jpcc.9b01722.

Simulation snapshots of the creation of polymer surface, Gd^{3+}-water structure RDF plots, density distribution, and PMF curves (PDF)

■ AUTHOR INFORMATION

Corresponding Author

*Phone: 91-512-259 6141 (office). Fax: 91-512-259 0104. E-mail: jayantks@iitk.ac.in.

ORCID

Anil Boda: 0000-0002-2984-0826

Sk. Musharaf Ali: 0000-0003-0457-0580

Jayant K. Singh: 0000-0001-8056-2115

Notes

The authors declare no competing financial interest.

■ ACKNOWLEDGMENTS

This work is supported by the Board of Research on Nuclear Sciences (BRNS), Department of Atomic Energy (DAE), and Government of India, sanctioned no: 36(1)/14/02/2015-BRNS/100. We are grateful to HPC, IIT Kanpur for the computational support. P.S. gratefully acknowledges the Science and Engineering Research Board (SERB), Department of Science and Technology (DST), Government of India, for the National Post-Doctoral Fellowship (PDF/2017/000121).

■ REFERENCES

(1) Berglund, M.; Wieser, M. E. Isotopic compositions of the elements 2009 (IUPAC Technical Report). *Pure Appl. Chem.* **2011**, *83* (2), 397−410.

(2) Sears, V. F. *Thermal-Neutron Scattering Lengths and Cross Sections for Condensed-Matter Research*; Report No. AECL-8490; Atomic Energy of Canada Ltd.: Chalk River, ON, Canada, 1984.

(3) Bianchi, A.; Calabi, L.; Corana, F.; Fontana, S.; Losi, P.; Maiocchi, A.; Paleari, L.; Valtancoli, B. Thermodynamic and structural properties of Gd (III) complexes with polyamino-polycarboxylic ligands: basic compounds for the development of MRI contrast agents. *Coord. Chem. Rev.* **2000**, *204* (1), 309−393.

(4) Raju, C. S. K.; Lück, D.; Scharf, H.; Jakubowski, N.; Panne, U. A novel solid phase extraction method for pre-concentration of gadolinium and gadolinium based MRI contrast agents from the environment. *J. Anal. At. Spectrom.* **2010**, *25* (10), 1573−1580.

(5) De Jong, N.; Draye, M.; Favre-Réguillon, A.; LeBuzit, G.; Cote, G.; Foos, J. Lanthanum (III) and gadolinium (III) separation by cloud point extraction. *J. Colloid Interface Sci.* **2005**, *291*, 303−306.

(6) Miranda, P., Jr; Zinner, L. B. Separation of samarium and gadolinium solutions by solvent extraction. *J. Alloys Compd.* **1997**, *249*, 116−118.

(7) Chitry, F.; Garcia, R.; Nicod, L.; Gass, J.-L.; Madic, C.; Lemaire, M. Separation of gadolinium (III) and lanthanum (III) by nanofiltration-complexation in aqueous medium. *J. Radioanal. Nucl. Chem.* **1999**, *240*, 931−934.

(8) Garcia, R.; Vigneau, O.; Pinel, C.; Lemaire, M. Solid−liquid lanthanide extraction with ionic-imprinted polymers. *Sep. Sci. Technol.* **2002**, *37*, 2839−2857.

(9) Besson, E.; Mehdi, A.; Van der Lee, A.; Chollet, H.; Reyé, C.; Guilard, R.; Corriu, R. J. P. Selective lanthanides sequestration based on a self-assembled organosilica. *Chem. - Eur. J.* **2010**, *16*, 10226−10233.

(10) Qadeer, R.; Hanif, J.; Saleem, M.; Afzal, M. Adsorption of gadolinium on activated charcoal from electrolytic aqueous solution. *J. Radioanal. Nucl. Chem.* **1992**, *159*, 155−165.

(11) Boda, A.; Deb, A. K. S.; Ali, Sk. M.; Shenoy, K. T.; Mohan, S. Molecular engineering of functionalized crown ether resins for the isotopic enrichment of gadolinium: from computer to column chromatography. *Mol. Sys. Des. Eng.* **2017**, *2*, 640−652.

(12) Boda, A.; Arora, S. K.; Deb, A. K. S.; Jha, M.; Ali, Sk. M.; Shenoy, K. T. Molecular modeling guided isotope separation of gadolinium with strong cation exchange resin using displacement chromatography. *Sep. Sci. Technol.* **2017**, *52*, 2300−2307.

(13) Zhang, A.; Kuraoka, E.; Hoshi, H.; Kumagai, M. Synthesis of two novel macroporous silica-based impregnated polymeric composites and their application in highly active liquid waste partitioning by extraction chromatography. *J. Chromotogr. A* **2004**, *1061* (2), 175−182.

(14) Pedersen, C. J. Cyclic polyethers and their complexes with metal salts. *J. Am. Chem. Soc.* **1967**, *89* (26), 7017−7036.

(15) De, S.; Boda, A.; Ali, S. M. Preferential interaction of charged alkali metal ions (guest) within a narrow cavity of cyclic crown ethers (neutral host): a quantum chemical investigation. *J. Mol. Struct.: THEOCHEM* **2010**, *941* (1−3), 90−101.

(16) Rogers, R. D.; Kurihara, L. K. F-Element/crown ether complexes. 4. Synthesis and crystal and molecular structures of $[MCl(OH_2)_2(18\text{-crown-}6)]Cl_2.2H_2O$ (M= samarium, gadolinium, terbium). *Inorg. Chem.* **1987**, *26*, 1498−1502.

(17) Alexandratos, S. D.; Stine, C. L. Synthesis of ion-selective polymer-supported crown ethers: a review. *React. Funct. Polym.* **2004**, *60*, 3−16.

(18) Wild, G. P.; Wiles, C.; Watts, P.; Haswell, S. J. The use of immobilized crown ethers as in-situ N-protecting groups in organic synthesis and their application under continuous flow. *Tetrahedron* **2009**, *65*, 1618−1629.

(19) Wiktorowicz, S.; Duchêne, R.; Tenhu, H.; Aseyev, V. Multi-stimuli responsive poly (azodibenzo-18-crown-6-ether)s. *Polym. Chem.* **2014**, *5*, 4693−4700.

(20) Gao, B.; Wang, S.; Zhang, Z. Study on complexation adsorption behavior of dibenzo-18-crown-6 immobilized on CPVA microspheres for metal ions. *J. Inclusion Phenom. Mol. Recognit. Chem.* **2010**, *68*, 475−483.

(21) Tapia, M. J.; Burrows, H. D.; García, J. M.; García, F.; Pais, A. A. C. C. Lanthanide ion interaction with a crown ether methacrylic polymer, poly (1, 4, 7, 10-tetraoxacyclododecan-2-ylmethyl methacrylate), as seen by spectroscopic, calorimetric, and theoretical studies. *Macromolecules* **2004**, *37*, 856−862.

(22) Rubio, F.; García, F.; Burrows, H. D.; Pais, A. A. C. C.; Valente, A. J. M.; Tapia, M. J.; García, J. M. Aqueous solution and solid state interactions of lanthanide ions with a methacrylic ester polymer bearing pendant 15-crown-5 moieties. *J. Polym. Sci., Part A: Polym. Chem.* **2007**, *45*, 1788−1799.

(23) Buenzli, J. C.G.; Pilloud, F. Complexes of lanthanoid salts with macrocyclic ligands. 36. Macrocyclic effect in lanthanoid complexes with 12-, 15-, 18-, and 21-membered crown ethers. *Inorg. Chem.* **1989**, *28*, 2638−2642.

(24) Van Veggel, F. C.J.M.; Reinhoudt, D. N. New, Accurate Lennard-Jones Parameters for Trivalent Lanthanide Ions, Tested on [18] Crown−6. *Chem. - Eur. J.* **1999**, *5*, 90−95.

DOI: 10.1021/acs.jpcc.9b01722
J. Phys. Chem. C 2019, 123, 12276−12285

(25) Villa, A.; Hess, B.; Saint-Martin, H. Dynamics and structure of Ln (III)− aqua ions: a comparative molecular dynamics study using ab initio based flexible and polarizable model potentials. *J. Phys. Chem. B* **2009**, *113*, 7270−7281.
(26) Kim, H.-S.; Chi, K.-W. Monte Carlo simulation study for QSPR of solvent effect on the selectivity of 18-crown-6 between Gd^{3+} and Yb^{3+} ions.". *J. Mol. Struct.: THEOCHEM* **2005**, *722*, 1−7.
(27) Sappidi, P.; Namsani, S.; Ali, Sk. M.; Singh, J. K. Extraction of Gd^{3+} and UO_2^{2+} ions using polystyrene grafted dibenzo crown ether (DB18C6) with octanol and nitrobenzene: A molecular eynamics study. *J. Phys. Chem. B* **2018**, *122*, 1334−1344.
(28) Sappidi, P.; Mir, S. H.; Singh, J. K. Effect of polystyrene length for the extraction of Gd^{3+} and UO_2^{2+} ions using dicyclohexano crown ether (DCH18C6) with octanol and nitrobenzene: A molecular dynamics study. *J. Mol. Liq.* **2018**, *271*, 166−174.
(29) *Materials Studio Modeling Environment*, Release 5.0; Accelrys Software Inc.: San Diego, CA, 2007.
(30) Frisch, M. J.; Trucks, G. W.; Schlegel, H. B.; Scuseria, G. E.; Robb, M. A.; Cheeseman, J. R.; Scalmani, G.; Barone, V.; Petersson, G. A.; Nakatsuji, H.; et al. *Gaussian 09*, revision D.01; Gaussian, Inc.: Wallingford, CT, 2009.
(31) Jorgensen, W. L.; Maxwell, D. S.; Tirado-Rives, J. Development and testing of the OPLS all-atom force field on conformational energetics and properties of organic liquids. *J. Am. Chem. Soc.* **1996**, *118*, 11225−11236.
(32) Jorgensen, W. L.; Chandrasekhar, J.; Madura, J. D.; Impey, R. W.; Klein, M. L. Comparison of simple potential functions for simulating liquid water. *J. Chem. Phys.* **1983**, *79*, 926−935.
(33) Darden, T.; York, D.; Pedersen, L. Particle mesh Ewald: An N·log (N) method for Ewald sums in large systems. *J. Chem. Phys.* **1993**, *98*, 10089−10092.
(34) Hess, B.; Bekker, H.; Berendsen, H. J.; Fraaije, J. G. LINCS: a linear constraint solver for molecular simulations. *J. Comput. Chem.* **1997**, *18*, 1463−1472.
(35) Pronk, S.; Páll, S.; Schulz, R.; Larsson, P.; Bjelkmar, P.; Apostolov, R.; Shirts, M. R.; Smith, J. C.; Kasson, P. M.; Van Der Spoel, D.; et al. GROMACS 4.5: a high-throughput and highly parallel open source molecular simulation toolkit. *Bioinformatics* **2013**, *29*, 845−854.
(36) Walsh, D. J.; Zoller, P. *Standard Pressure-Volume-Temperature Data for Polymers*; Technomic Publishing Company: Lancaster, PA, 1995; p 412.
(37) Bekele, S.; Tsige, M. Interfacial properties of oxidized polystyrene and its interaction with water. *Langmuir* **2013**, *29*, 13230−13238.
(38) Kumar, S.; Rosenberg, J. M.; Bouzida, D.; Swendsen, R. H.; Kollman, P. A. The weighted histogram analysis method for free-energy calculations on biomolecules. I. The method. *J. Comput. Chem.* **1992**, *13*, 1011−1021.
(39) Roux, B. The calculation of the potential of mean force using computer simulations. *Comput. Phys. Commun.* **1995**, *91*, 275−282.
(40) Hub, J. S.; De Groot, B. L.; Van Der Spoel, D. g_wham: A free weighted histogram analysis implementation including robust error and autocorrelation estimates. *J. Chem. Theory Comput.* **2010**, *6*, 3713−3720.
(41) McKay, G.; Blair, H. S.; Gardner, J. R. Adsorption of dyes on chitin. 1. Equilibrium studies. *J. Appl. Polym. Sci.* **1982**, *27*, 3043−3057.
(42) Ohtaki, H.; Radnai, T. Structure and dynamics of hydrated ions. *Chem. Rev.* **1993**, *93*, 1157−1204.
(43) Clavaguera, C.; Calvo, F.; Dognon, J. P. Theoretical study of the hydrated Gd^{3+} ion: Structure, dynamics, and charge transfer. *J. Chem. Phys.* **2006**, *124*, 074505.
(44) Latrous, H.; Oliver, J. Self-diffusion coefficients and structure of the trivalent transplutonium ion curium and gadolinium in aqueous solution. *J. Radioanal. Nucl. Chem.* **1992**, *156*, 291−296.
(45) Kommu, A.; Velachi, V.; Cordeiro, M. N. D. S.; Singh, J. K. Removal of Pb (II) ion using PAMAM dendrimer grafted graphene and graphene oxide surfaces: A molecular dynamics study. *J. Phys. Chem. A* **2017**, *121*, 9320−9329.

DOI: 10.1021/acs.jpcc.9b01722
J. Phys. Chem. C 2019, 123, 12276−12285